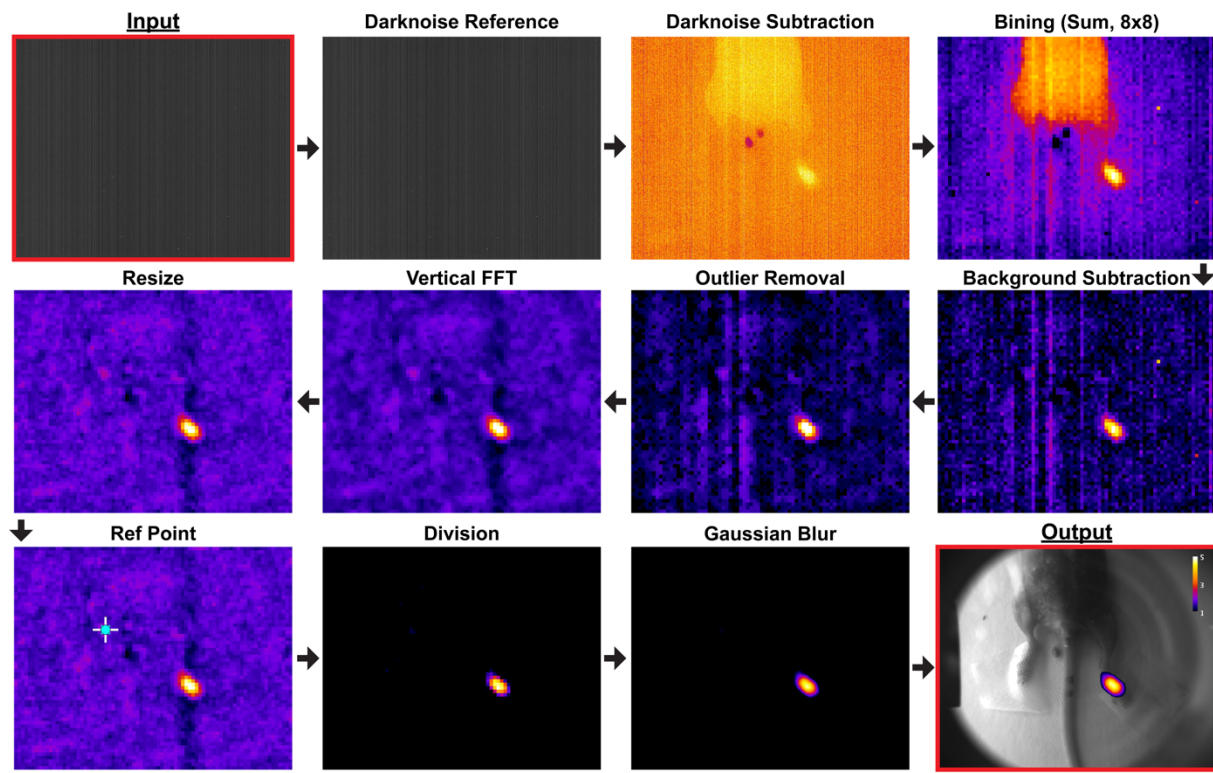


## **Supplemental Material: Shortwave infrared detection of medical radioisotope Cerenkov luminescence**

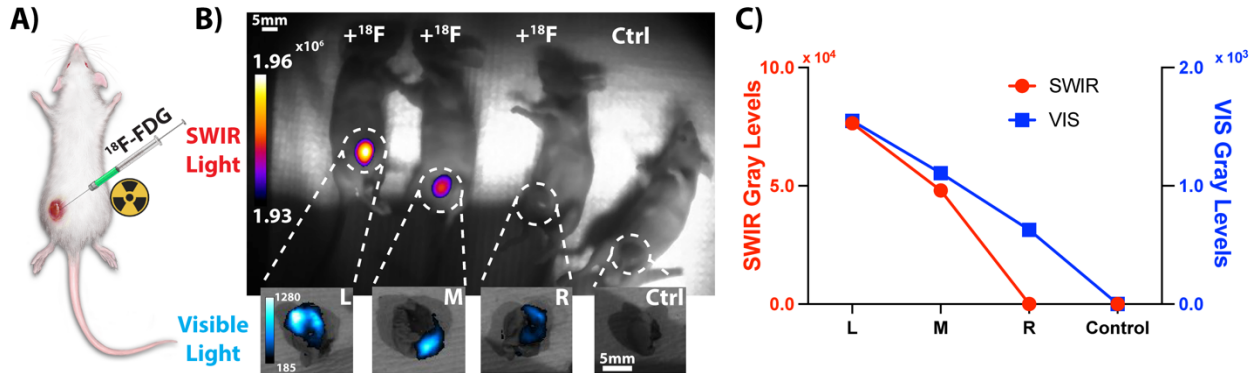
Benedict E. Mc Larney<sup>1,2</sup>, Qize Zhang<sup>1,2</sup>, Edwin C. Pratt<sup>1,2</sup>, Magdalena Skubal<sup>1,2</sup>, Elizabeth Isaac<sup>1,2</sup>, Hsiao-Ting Hsu<sup>1,2</sup>, Anuja Ogirala<sup>1,2</sup>, Jan Grimm<sup>1,2,3,4,5,\*</sup>

1. Molecular Pharmacology Program, Memorial Sloan Kettering Cancer Center, New York, NY, USA
2. Molecular Imaging Therapy Service, Memorial Sloan Kettering Cancer Center, New York, NY, USA
3. Pharmacology Program, Weill Cornell Medical College, New York, NY USA
4. Department of Radiology, Memorial Sloan Kettering Cancer Center, New York, NY, USA
5. Department of Radiology, Weill, Cornell Medical Center, New York, NY, USA

\*. Corresponding author: Jan Grimm - [grimmj@mskcc.org](mailto:grimmj@mskcc.org)

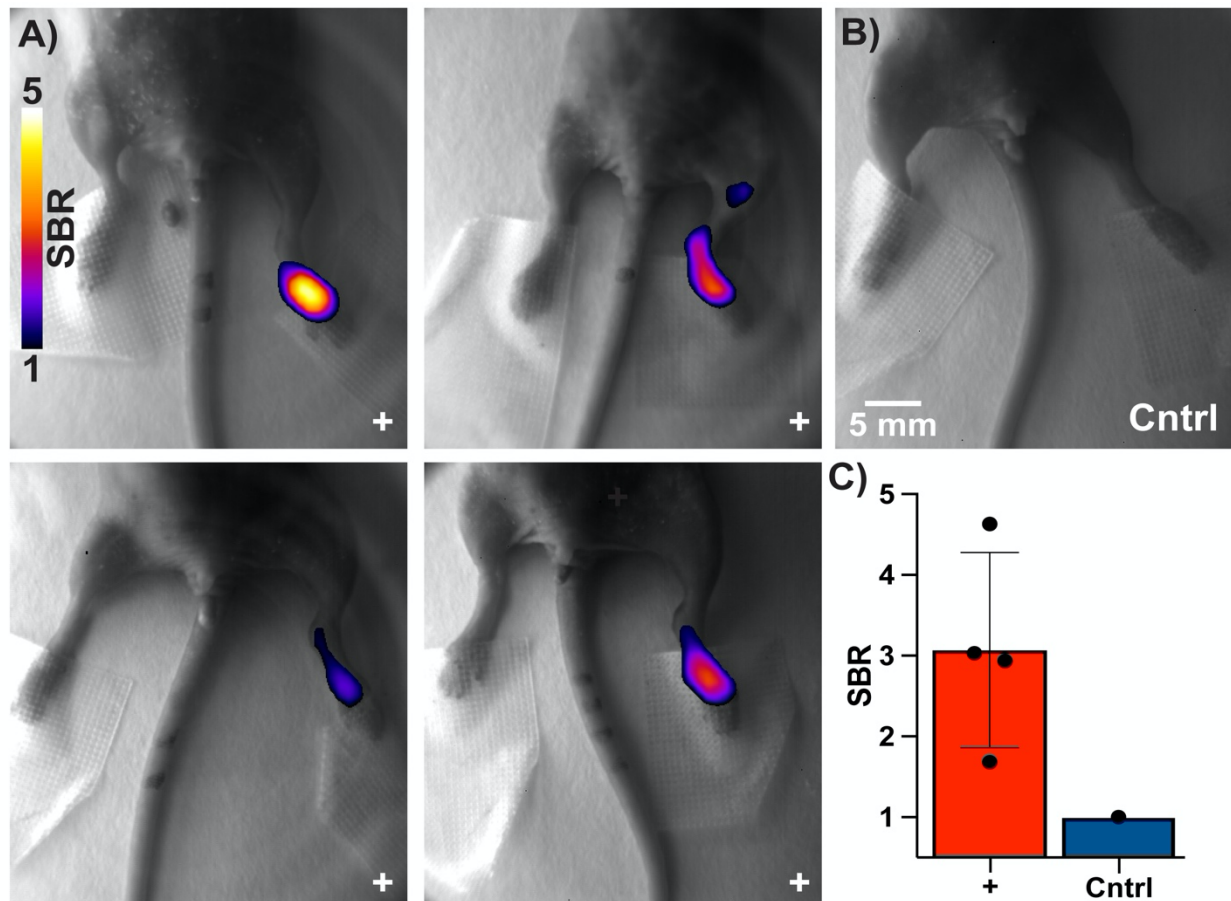


**Supplemental Figure 1. Image processing pipeline for *in vivo* SWIR CLI.** Images are presented from input to output including all necessary processing steps to generate the *in vivo* images. The input is based on a summation of  $n = 90$  16-bit, 10s images (900s/15 mins total acquisition time). Post darknoise subtraction images were processed in 32-bit formats. Gaussian blur was applied with a sigma of 3.



**Supplemental Figure 2. Ex vivo SWIR CLI & VIS CLI comparison of 4T1 xenografted mice intratumorally injected with clinical  $^{18}\text{F}$ -FDG** A) Euthanized mice were injected with  $^{18}\text{F}$ -FDG directly into the tumor. B) The corresponding image of 3 mice injected with  $^{18}\text{F}$ -FDG and one control mouse. Top, SWIR CL image, bottom VIS CL images of resected tumors (IVIS) C) Gray Value Cerenkov intensities for each tumor in both SWIR and visible light modalities (background subtracted). For B) & C) SWIR images and data points are summations from  $n = 360$  technical replicates and visible images are from a single acquisition from  $n = 3$   $^{18}\text{F}$ -FDG intratumorally injected mice and  $n = 1$  non-injected mouse (biological replicates).

Initial experiments assessed the application of preclinical SWIR CLI with  $^{18}\text{F}$ -FDG. The inherent noise in the SWIR sensor and lower CL intensity of  $^{18}\text{F}$  ( $\beta$  average 0.25 MeV), required that  $^{18}\text{F}$ -FDG be injected on the order of a few mCi to be detected in a murine setting. Experimentation in this format spatially concentrated the source further enabling detection (intratumoral injection, see Supplemental Figure 2A). It should be noted this is not representative of conventional CLI. Imaging was carried out post euthanasia and following the immediate injection of  $^{18}\text{F}$ -FDG into the tumor. As shown in Supplemental Figure 2B, three mice were administered  $^{18}\text{F}$ -FDG (with varying amounts up to 4.5 mCi). The fourth mouse received no injection (negative control). Mice were imaged over the course of an hour (360 frames, 10s each) with SWIR CL detected in two mice. Tumors were resected post SWIR CLI and imaged on a conventional VIS CLI system (IVIS), see Supplemental Figure 2B, bottom row. The corresponding gray values are plotted for both modalities in Supplemental Figure 2C. In the case of the left (L), middle (M) and control (Ctrl) mice the values are in close agreement.



**Supplemental Figure 3. In vivo SWIR CLI detection of  $^{90}\text{Y}$  labeled SiNPs three hours post injection into the footpad** **A)** Images of mice injected (+) with  $^{90}\text{Y}$  labeled SiNPs ( $\sim 200 \mu\text{Ci}$  per mouse). **B)** Image of a control mouse without any injection. **C)** Quantified values of injected ( $n = 4$ ) vs control mice ( $n = 1$ ). All images are shown in respective signal to background ratios (SBR). A, Top left and Cntrl mouse are the same image as shown in Main Figure 8.